Proceedings of the ASME 2020 39th International Conference on Ocean, Offshore and Arctic Engineering
OMAE2020
June 28-July 3, 2020, Fort Lauderdale, FL, USA

OMAE2020-18467

MODELING OF A SHARED MOORING SYSTEM FOR A DUAL-SPAR CONFIGURATION

Guodong Liang
Department of Engineering Sciences
University of Agder
N-4898 Grimstad, Norway

Karl Merz
Sintef Energy Research
N-7034 Trondheim, Norway

Zhiyu Jiang
Department of Engineering Sciences
University of Agder
N-4898 Grimstad, Norway

ABSTRACT

As floating wind turbines become more technically mature, the development of floating wind farms is under way. Cost-effective solutions are desired to reduce the mooring costs. The concept of a shared mooring system has been proposed for this purpose. This work presents a method to model the shared mooring system for a dual-spar configuration. By applying the theory in elastic catenary of cable structures, a shared line can be modelled. To verify the method, a dual-spar system is modelled in a multibody simulation tool, in which two floating wind turbines are connected via a shared line. Static analyses are performed by using the present method and the simulation tool. Further, a sensitivity study is applied to the shared line properties. Different mooring line properties have been investigated. The influence of the shared line properties is shown on the mooring restoring properties of the dual-spar system. The present modeling method can be applied in the preliminary design stage of shared mooring systems.

INTRODUCTION

Wind energy plays an important role in energy transformation happening worldwide. The growth of wind energy is noticeable. Since 1990, wind energy has grown with an average annual rate of 23.4%, while the average annual rate of total renewable energy growth since 1990 is just 2.0% [1]. There are several advantages to develop offshore wind farms. Compared with land-based wind farms, offshore wind farms experience stronger and more stable wind, and cause less visual impact. The space resource is also much more abundant in the ocean. Therefore, it is beneficial to develop offshore wind farms. Bottom-fixed offshore wind farms have been widely deployed and commercialized. However, for places with limited access to shallow water areas, where a bottom-fixed offshore wind farm is no longer applicable, the floating wind farm is an alternative. As the next wave of wind energy, the design of floating wind farms has attracted increasing research interests.

The first floating wind farm, Hywind Scotland, was commissioned in 2017 [2]. However, to achieve large-scale deployment, floating wind energy needs to be cost-competitive in the energy market. Cost reductions of floating wind farms can be achieved on two levels. On the wind turbine level, the probabilistic design approach can be applied, followed by design optimization. On the wind farm level, layout optimization is a way to cut costs. A mooring system is designed to control the position and motion of a floating wind turbine. For floating wind farms, long mooring lines need to be used to fulfill the requirements of station-keeping

purpose, which increases the costs of mooring systems. A shared mooring system is one of the novel designs which brings the potential to reduce the costs in mooring systems. With a shared mooring system, wind turbines are connected by shared lines, which reduces the mooring line usage. The number of anchors is also reduced, which brings reductions in costs related to site investigation and anchor installations. However, since individual wind turbines are coupled by the shared lines, extra complexity is introduced to the dynamic behaviors of the floating system. It is necessary to assess the influence of the shared mooring system and demonstrate its feasibility in real applications.

A shared mooring system was studied by Gao and Moan for wave energy converters (WECs) [3]. The time-domain method was applied to analyze the dynamic behaviors of a shared mooring system for nine WECs. The results indicated that individual mooring was more feasible than the shared mooring system. Goldschmidt and Muskulus investigated the dynamic properties and the cost-saving potential of shared mooring systems [4]. Frequency-domain method and time-domain method were applied for simplified models with different configurations. The results revealed the great potential of cost reductions by applying a shared mooring system. However, increasing displacements were reported when the number of wind turbines increased. The dynamics of a square-shaped four-turbine model with a shared mooring system was studied by Hall and Connolly [5]. Coupled time-domain simulations were performed. Complex restoring properties of the shared mooring system were captured. Without contact with the seabed, a greater tendency for resonance was found for shared lines. In the following research by Connolly and Hall, the shared mooring system was analyzed for a four-turbine pilot scale floating wind farm [6]. Different configurations of the shared mooring system and different water depths were studied. The platform displacements, mooring tensions, and costs were checked. A design algorithm was presented for the shared mooring system.

Inspired by the aforementioned research, this paper focuses on the modeling of a shared mooring system for a dual-spar configuration. A method from cable structures is introduced and applied to model the shared line. The method is verified by Finite Element (FE) modeling in static analyses. A sensitivity study is further applied for the shared line properties. The influence of the shared line on the mooring restoring properties of the system is captured. The presented method is applicable to the preliminary design of a shared mooring system.

METHODOLOGY

Mooring lines are connected to a wind turbine through fairleads. Another end of a mooring line is fixed on the seabed by an anchor. When a wind turbine is away from its equilibrium position, the resulting mooring restoring forces acting on the wind turbine move it back. The maximum tension loads in individual mooring lines are important in the design of mooring systems. While for floating wind turbines, it is the total mooring force acting on the wind turbine that contributes to its motion. For both cases, accurate modeling of mooring lines is important.

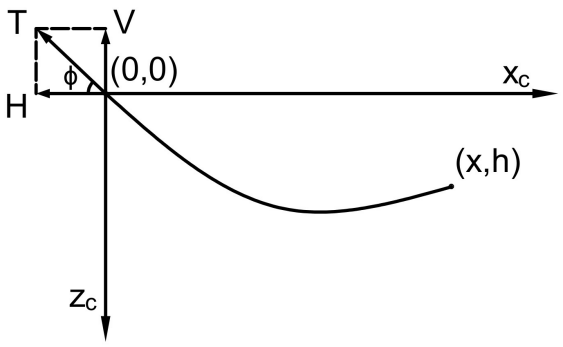

FIGURE 1. THE CATENARY PLANE OF A SHARED LINE DEFINED IN IRVINE'S MODELING METHOD

The catenary plane of a mooring line is the vertical plane defined by its catenary line shape. The catenary plane of a shared line is illustrated in Fig. 1. Faltinsen presented a method to model the mooring line as an elastic cable line [7]. An assumption is made that the bending stiffness of a mooring line could be neglected. This is reasonable for mooring chains and steel wire ropes with large curvature [7]. The dynamic effects in the mooring line and the effects of current forces acting on the mooring line are also neglected. The origin of the catenary plane is set as the touchdown point of the mooring line in the method presented by Faltinsen. By solving a group of elastic catenary equations, Eqn. (1) and Eqn. (2), the position of the fairlead in the catenary plane can be computed for given mooring tension.

$$x = \frac{H}{\omega} log(\frac{\sqrt{H^2+V^2}+V}{H}) + \frac{H}{EA} l_s \tag{1}$$

$$h = \frac{H}{\omega}\left[\frac{1}{cos\phi} - 1\right] + \frac{1}{2}\frac{\omega}{EA} l_s^2 \tag{2}$$

Where:

- x and h are the horizontal and vertical distance between the fairlead and the touchdown point.
- H and V are the horizontal and vertical components of mooring tension T at the fairlead.
- ϕ is the angle between the mooring tension T and its horizontal component H.

- ω is the weight per unit length of the mooring line in the water.
- EA is the extensional stiffness, with E as the elastic modulus of the line and A as the cross-sectional area of the line.
- l_s is the length of the line hanging in the water.

In practice, the positions of the fairlead and the anchor point are usually known, while the mooring tension needs to be computed. Since current forces acting on the mooring line are neglected, the vertical component of the mooring tension is purely caused by the submerged weight of hanging part of the mooring line l_s. With an initial guess of the value of l_s, x and h in the catenary plane can be determined. By solving Eqn. (1) and Eqn. (2) numerically, H and V are obtained. V is then used to update the value of l_s. After iterations, the value of l_s converges. Then the touchdown point is located, and the mooring tension can be obtained.

For modeling of a shared line, Faltinsen's method is applicable if the two fairleads are on the same level. In this case, the line shape of the shared line is symmetrical and it can be modelled as two single lines connected at the sagging point. In cases where different levels are found for two fairleads and the line shape is unsymmetrical, Faltinsen's method is not applicable since the number of unknown variables exceeds the number of equations. Instead, the theory of elastic catenary for hanging cable structures presented by Irvine is applicable [8]. The same assumptions as in the method presented by Faltinsen should be made to apply Irvine's method. By setting one end of the shared line as the origin of the catenary plane, the elastic catenary equations Eqn. (3) and Eqn. (4) are applied. Some of the variables in Eqn. (3) and Eqn. (4) are illustrated in Fig. 1. x_c and z_c are the horizontal and vertical axes in the catenary plane.

$$x = \frac{Hs}{EA} + \frac{H}{\omega}\left[sinh^{-1}(\frac{V}{H}) - sinh^{-1}(\frac{V-\omega s}{H})\right] \tag{3}$$

$$h = \frac{\omega s^2}{EA}\left[\frac{V}{\omega s} - \frac{1}{2}\right] + \frac{H}{\omega}\left[\sqrt{1+\left(\frac{V}{H}\right)^2} - \sqrt{1+\left(\frac{V-\omega s}{H}\right)^2}\right] \tag{4}$$

Where:

- x and h are the horizontal and vertical distance between the origin of the catenary plane and the other end of the shared line.
- s is the total unstrained length of the shared line.

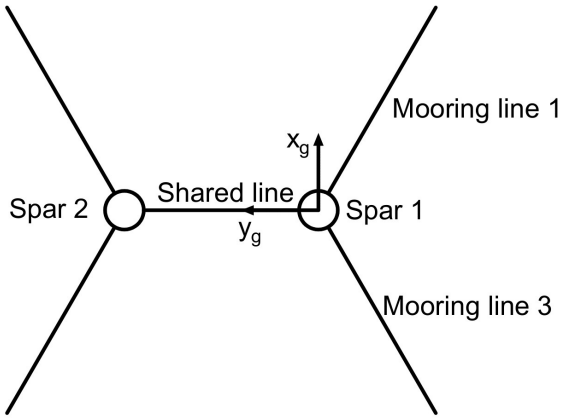

FIGURE 2. TOP VIEW OF THE INITIAL CONFIGURATION OF THE DUAL-SPAR SYSTEM

Other variables in Eqn. (3) and Eqn. (4) have the same definitions as in Eqn. (1) and Eqn. (2). With given coordinates of two fairleads, the catenary plane can be defined, and mooring tension is computed by solving Eqn. (3) and Eqn. (4) numerically. It is also possible to compute the shape of the shared line in the catenary plane by introducing the Lagrangian coordinate in the derivation. Details can be found in [8]. The method presented by Irvine is applicable to a single mooring line as well. Considering the touchdown point as the second end and the hanging part of the mooring line as an independent line, the application is then similar to the shared line. Since the position of the touchdown point is usually unknown before the analysis, an initial guess of the length of the hanging part can be made. After the vertical component of the mooring tension is computed, the initial guess is updated. The calculations converge after some iterations, and the touchdown point is located.

CASE STUDY

A case study is performed to verify the modeling method. A model of a dual-spar system is established in the DNV GL simulation tool package [9–11]. The NREL 5MW reference wind turbine and the OC3 spar floating system have been modelled [12, 13]. First, hydrodynamic analysis has been performed for a dual-spar panel model in WADAM, a general wave analysis program [9]. From the WADAM analysis, hydrodynamic properties, like wave force transfer functions and retardation functions with hydrodynamic couplings, are obtained. They are imported and implemented in the model of the dual-spar structure in SIMA

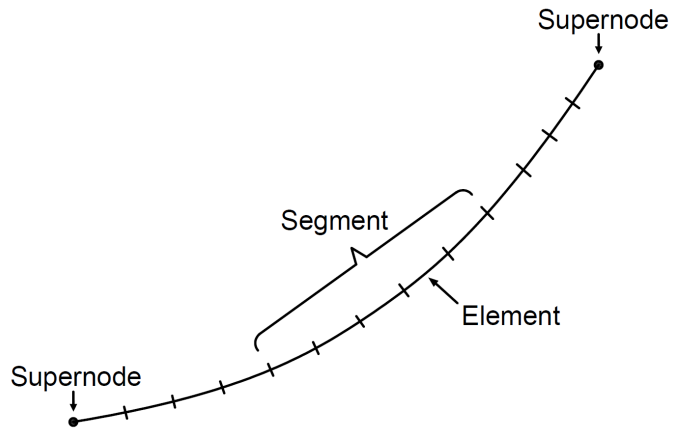

FIGURE 3. MODELING OF SLENDER STRUCTURES IN RIFLEX

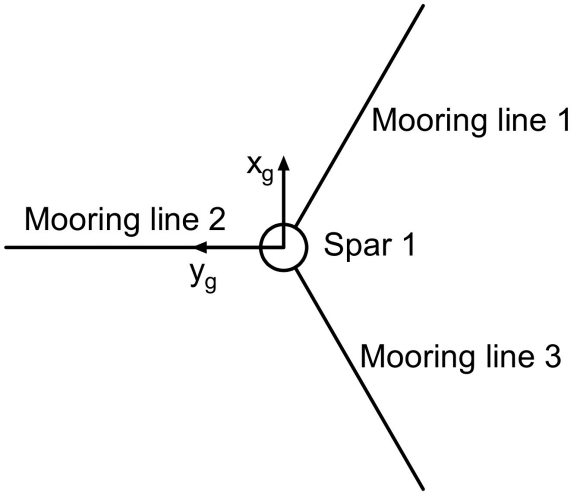

FIGURE 4. TOP VIEW OF THE INITIAL CONFIGURATION OF A SPAR FLOATING WIND TURBINE

workbench, a simulation tool for marine operations and floating systems [10, 11]. A top view of the dual-spar system is given in Fig. 2.

Wind turbines and spar floaters are modelled according to [12, 13]. The upwind wind turbines are placed with shafts along the x_g-axis in the global coordinate system and facing its negative direction. The shared line is aligned with the sway direction y_g in the current model, since no interactions in the wind or waves are considered in static analyses. In dynamic analyses, when the interactions need to be considered, structural configurations with

TABLE 1. SHARED LINE PROPERTIES: MOORING CHAIN

Property	OC3	Chain 1	Chain 2	Chain 3
Diameter [mm]	90	50	60	70
Mass density [kg/m]	77.71	50.00	72.00	98.00
Weight in water [N/m]	698.09	451.01	649.46	883.99
Extensional stiffness [N]	3.84E+08	2.36E+08	3.38E+08	4.57E+08
Maximum breaking load [N]	-	3.20E+06	4.52E+06	6.02E+06

TABLE 2. SHARED LINE PROPERTIES: STEEL WIRE ROPE

Property	OC3	Wire 1	Wire 2	Wire 3
Diameter [mm]	90	100	120	140
Sheath thickness [mm]	-	10	10	10
Mass density [kg/m]	77.71	52.24	73.98	99.45
Weight in water [N/m]	698.09	398.75	571.00	773.41
Extensional stiffness [N]	3.84E+08	9.35E+08	1.32E+09	1.78E+09
Maximum breaking load [N]	-	1.04E+07	1.49E+07	2.04E+07

different alignments should be investigated. Two single mooring lines are connected to each wind turbine through fairleads. The mooring system properties of OC3 Hywind have been used to model single mooring lines. It should be noticed that the mooring line properties are weighted-average properties of an equivalent homogeneous line [13]. Multi-segment mooring lines are expected in the original design of Hywind Demo. As illustrated in Fig. 3, slender structures are modelled in the RIFLEX module of SIMA workbench [11]. The fairlead and the anchor point are modelled as supernodes to define both ends of a mooring line. Each mooring line consists of FEs with pre-defined cross-section properties. By defining different cross sections, modeling of a multi-segment mooring line with different materials is possible. In the initial condition, two spar floaters are placed with a distance of 750 m along the y_g-axis, which is six times of the wind turbine diameter. Due to the self-weight of the shared line, two wind turbines are driven towards each other for a short distance along the y_g-axis in the static condition. In the current model, 30 bar elements have been used in the FE modeling of each single mooring line, with a length of 902.2 m [13]. The shared line is modelled with 30 bar elements between two fairleads, with a total length of 739.6 m. The assumptions to apply the elastic catenary modeling method are implemented. A single floating wind turbine is modelled for comparison. The mooring system of the single floating wind turbine is modelled based on [13]. A top view of the single floating wind turbine is shown in Fig. 4.

TABLE 3. TENSION CALCULATION FOR MOORING LINE 1 IN THE DUAL-SPAR SYSTEM, LINE PROPERTIES FROM [13]

Result	RIFLEX	Irvine	Difference with RIFLEX [%]
T [N]	9.784E+05	9.899E+05	1.175
H [N]	8.102E+05	8.158E+05	0.691
V [N]	5.485E+05	5.607E+05	2.224
ϕ [deg]	34.096	34.503	1.194
Elongation [-]	2.248E-03	2.284E-03	1.601

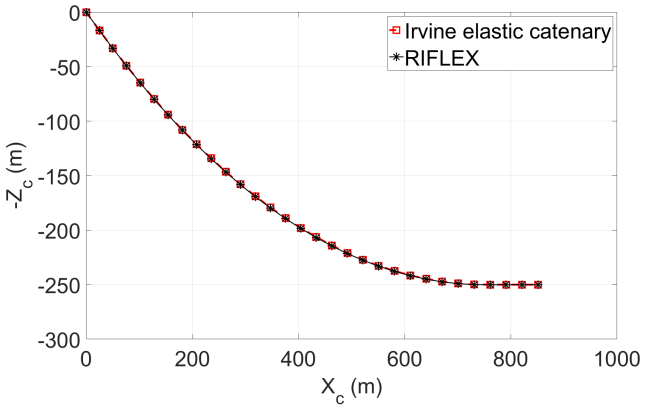

FIGURE 5. LINE SHAPE IN THE CATENARY PLANE FOR MOORING LINE 1 IN THE DUAL-SPAR SYSTEM

A sensitivity study is performed for the shared line properties. Both R5 studless mooring chain, and spiral strand and sheathed mooring steel wire rope are investigated. Shared lines with different diameters are modelled. The line properties are summarized in Tab. 1 and Tab. 2, together with the line properties from [13]. The line properties of the mooring chains and the steel wire ropes are obtained from offshore standards [14–16] and commercial data.

RESULTS

Static analysis is performed in the SIMA workbench for the dual-spar model. The static positions of fairleads obtained from the analysis are taken as initial inputs when applying the modeling method based on Irvine's elastic catenary theory. The results of the comparison and the sensitivity study are listed in the following sections.

TABLE 4. TENSION CALCULATION FOR THE SHARED LINE AT THE FAIRLEAD ON SPAR 1, LINE PROPERTIES FROM [13]

Result	RIFLEX	Irvine	Difference with RIFLEX [%]
T [N]	8.547E+05	8.573E+05	0.304
H [N]	8.174E+05	8.175E+05	0.012
V [N]	2.496E+05	2.582E+05	3.446
ϕ [deg]	16.980	17.525	3.210
Elongation [-]	2.162E-03	2.162E-03	0

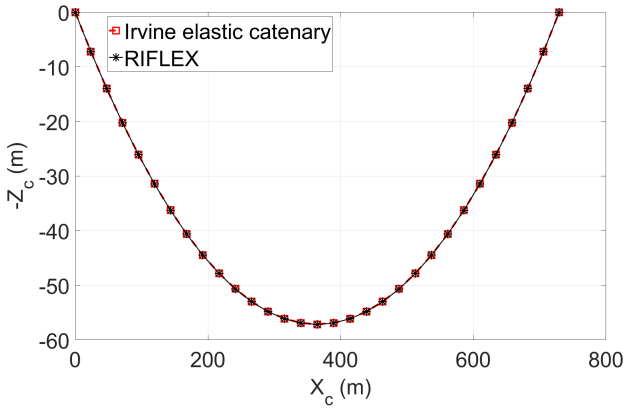

FIGURE 6. LINE SHAPE IN THE CATENARY PLANE FOR THE SHARED LINE

Comparison with FE modeling in RIFLEX

With the positions of fairleads from static analysis as inputs, the present modeling method is applied to compute the line tension at the fairlead and the line shape in the catenary plane. Mooring line properties from [13] are used. The results from FE modeling in RIFLEX are taken as references. The results of tension calculations for mooring line 1 are summarized in Tab. 3. The line shape in the catenary plane is plotted in Fig. 5. The results of tension calculations for the shared line are presented in Tab. 4 and the line shape comparison is shown in Fig. 6.

For both the single mooring line and the shared line, good agreements are achieved for the tension calculations and line shapes. The feasibility is demonstrated for the present modeling method.

Comparison of Line Tension

In the following sensitivity studies, only the modeling method based on Irvine's elastic catenary theory is applied.

The relationships between the offset of Spar 1 and the ten-

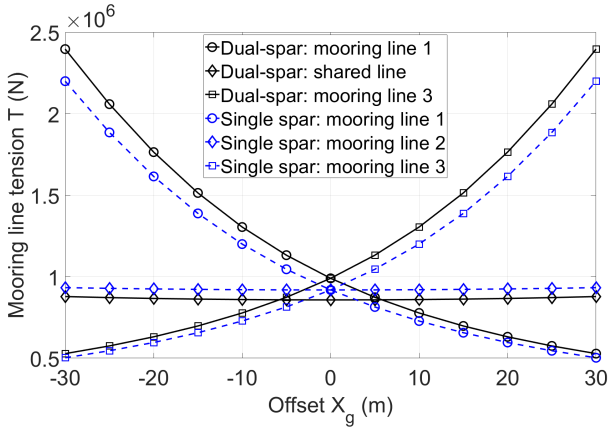

FIGURE 7. RELATIONSHIP BETWEEN LINE TENSION AND OFFSET X_g

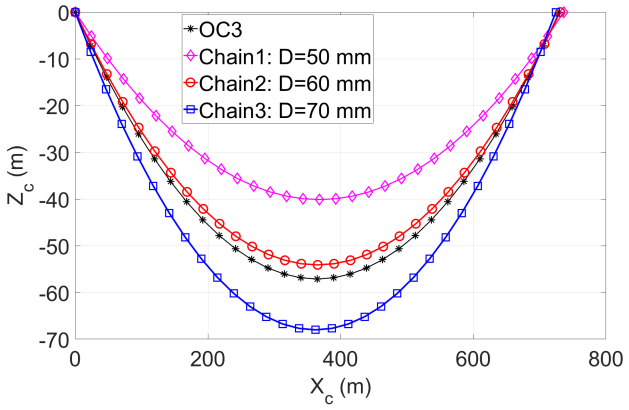

FIGURE 9. LINE SHAPE IN THE CATENARY PLANE FOR DIFFERENT MOORING CHAINS

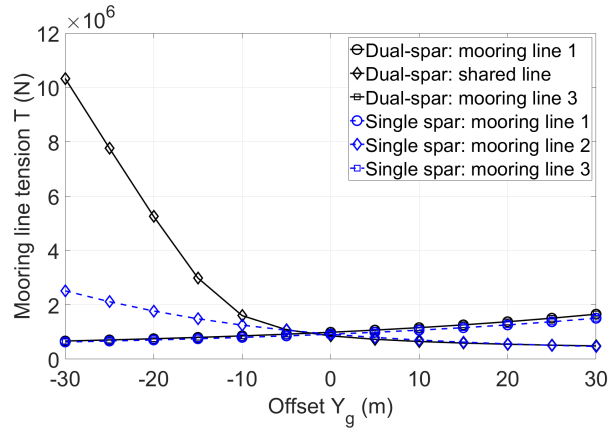

FIGURE 8. RELATIONSHIP BETWEEN LINE TENSION AND OFFSET Y_g

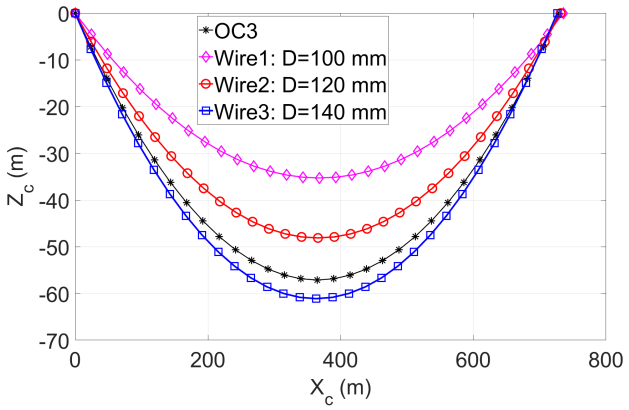

FIGURE 10. LINE SHAPE IN THE CATENARY PLANE FOR DIFFERENT STEEL WIRE ROPES

sion in each line are investigated in the directions of x_g and y_g; see Fig. 2 and Fig. 4. Spar 2 is fixed in six degrees of freedom (DOFs). Results of the dual-spar system are compared with those of the single floating wind turbine and are presented in Fig. 7 and Fig. 8. The properties of mooring lines investigated are the same as in [13]. By comparing the mooring tension and the maximum breaking loads (MBLs) of the shared line with different line properties, a range of -30 m to +30 m is chosen for the offset in the plots.

Due to the symmetry of the structural configuration about y_g-axis, the tension in mooring line 1 and mooring line 3 is symmetrical about $X_g = 0$ in Fig. 7. It is noticed that maximum tension is found in the single mooring lines in Fig. 7. While in Fig. 8, maximum tension is achieved in the shared line for the dual-spar system and mooring line 2 for the single floating wind turbine. Although the MBL of mooring lines is not specified in [13], the tension in the shared line at $Y_g = -30\ m$ should be quite close to the MBL. Therefore, the relationship between the tension in the shared line and the offset Y_g of Spar 1 is investigated for different line properties. The line shapes in the catenary plane for shared lines with different line properties are plotted and compared with the shared line modelled with OC3 line properties. From Fig. 9 and Fig. 10, it can be seen that the sagging extent of the shared lines relates to the weight in water. The horizontal distance between two spars also varies for different line properties since the total weight of the shared line differs. The tension in the shared line at the fairlead is computed against the offset of Spar 1 along the y_g-axis for different line properties. The results are presented in Fig. 11 for mooring chains and Fig. 12 for steel wire ropes. Nonlinearity is shown in the relationships

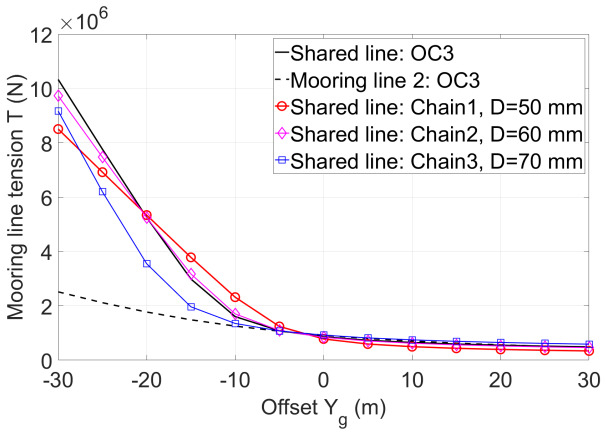

FIGURE 11. TENSION IN THE SHARED LINE FOR DIFFERENT MOORING CHAINS

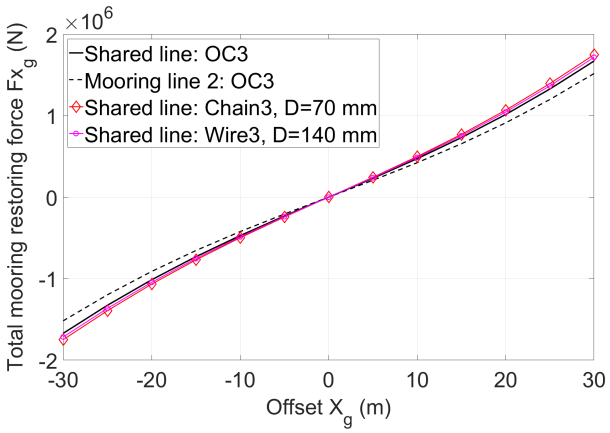

FIGURE 13. MOORING RESTORING CURVE OF SPAR 1 IN THE SURGE DIRECTION WITH SPAR 2 FIXED IN 6 DOFS

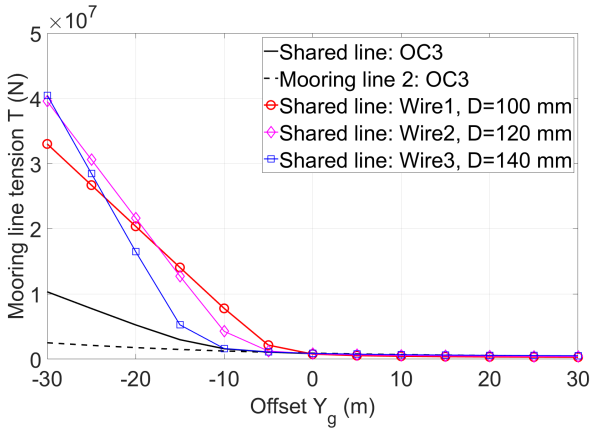

FIGURE 12. TENSION IN THE SHARED LINE FOR DIFFERENT STEEL WIRE ROPES

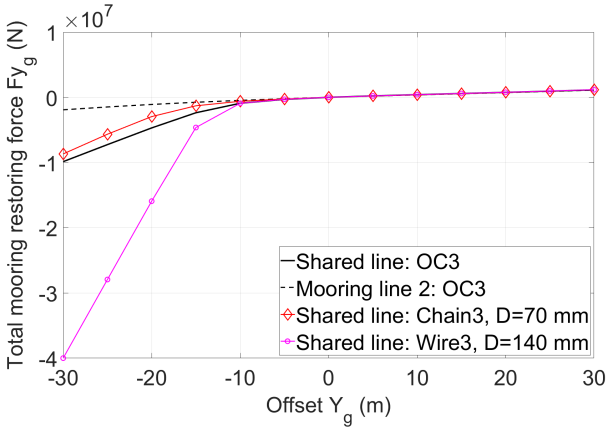

FIGURE 14. MOORING RESTORING CURVE OF SPAR 1 IN THE SWAY DIRECTION WITH SPAR 2 FIXED IN 6 DOFS

between the line tension and the offset Y_g especially when Spar 1 moves in the negative direction of y_g-axis and the shared line is tightened. In Fig. 11 and Fig. 12, when Spar 1 has a large negative offset Y_g, the tension in the shared lines exceeds the MBLs stated in Tab. 1 and Tab. 2 for all line properties. Therefore, it is of interest to know what the distance between the spar floating wind turbines can be in different operational conditions.

Comparison of Total Mooring Restoring Force

Since the tension in each line can be computed by the present modeling method, the total mooring restoring forces acting on wind turbines can be known. The total mooring restoring forces on Spar 1 are computed from tension acting on each fairlead. With Spar 2 fixed in 6 DOFs, the relationships between the total mooring restoring force acting on Spar 1 and the offset of Spar 1 along the x_g- and y_g-axes are investigated respectively. A comparison is made between the dual-spar system and the single floating wind turbine. Results are also plotted for the structural configurations in which the shared line is modelled with Chain 3 (Tab. 1) and Wire 3 (Tab. 2), respectively. Chain 3 and Wire 3 have the maximum mass properties and MBLs among others.

In Fig. 13, the relationship between the displacement of Spar 1 in the x_g-direction and the total mooring force is shown. From Fig. 13, it can be seen that the total mooring restoring effect in the surge direction is not sensitive to the design of the shared line. For different line properties of the shared line, the difference in mooring restoring force is not significant. This is reasonable since in the surge motion of Spar 1, the line tension in two single mooring lines is larger than the tension in the shared line, as shown in Fig. 7. The surge direction is also nearly perpendicular

to the catenary plane of the shared line, which makes the tension in the shared line contributes much less than the other two mooring lines. Even with an offset of 30 m, the distance is not large compared with the distance between the two wind turbines. However, it is obvious that the shared mooring system changes the restoring effects on Spar 1, compared with the results of the single floating wind turbine.

The relationship between the displacement of Spar 1 in the y_g-direction and the total mooring force is presented in Fig. 14. In Fig. 14, the influence of the shared line on the mooring restoring effects of Spar 1 is captured. When Spar 1 has a positive offset in the y_g-direction, the difference is not significant since the shared line gets loose and the mooring restoring effects are dominated by the other two single mooring lines. When Spar 1 has a negative offset in the y_g-direction, the shared line is strained, and the tension in the shared line becomes dominant, as shown in Fig. 8. From Fig. 14, it is clear that the mooring restoring effects of Spar 1 in the sway direction is significantly changed by the shared line, compared with the results from the single floating wind turbine.

CONCLUSION

Though a shared mooring system brings the possibility of cost reductions for floating wind farms, the additional complexity it introduces to the dynamic behaviors of the system needs to be addressed. For this purpose, a method to model the shared mooring system has been presented in this paper. A model of a dual-spar system has been established in the simulation tool SIMA workbench. The simulation results have verified the feasibility of the modeling method introduced. The influence of the shared line properties on the mooring restoring effects has been investigated through a sensitivity study. Different line properties have been generated and applied in shared line modeling. Comparisons have been made to the configuration of a single floating wind turbine. It has been revealed that the shared line has a significant influence on the mooring restoring effects in the sway DOF of the coupled floating system.

Static analysis has been performed in the current work. Since the described modeling method is also applicable in dynamic analysis, it would be interesting to investigate how the dynamic characteristics of the system can be influenced by the shared mooring system in future.

ACKNOWLEDGMENT

The authors acknowledge the financial support from the Research Council of Norway granted through the Department of Engineering Sciences, University of Agder.

The first author would like to thank Professor Erin Bachynski at the Norwegian University of Science and Technology for her help in SIMA modeling.

REFERENCES

[1] International Energy Agency, 2019. *Renewables Information 2019: Overview*.

[2] Hill, J. S., 2018. "Hywind scotland, world's first floating wind farm, performing better than expected". *Sustainable Enterprises Media, Inc,* ***16***.

[3] Gao, Z., and Moan, T., 2009. "Mooring system analysis of multiple wave energy converters in a farm configuration". In Proceedings of the 8th European Wave and Tidal Energy Conference, Uppsala, Sweden, pp. 7–10.

[4] Goldschmidt, M., and Muskulus, M., 2015. "Coupled mooring systems for floating wind farms". *Energy Procedia,* ***80***, pp. 255–262.

[5] Hall, M., and Connolly, P., 2018. "Coupled dynamics modelling of a floating wind farm with shared mooring lines". In ASME 2018 37th International Conference on Ocean, Offshore and Arctic Engineering, Madrid, Spain, American Society of Mechanical Engineers Digital Collection.

[6] Connolly, P., and Hall, M., 2019. "Comparison of pilot-scale floating offshore wind farms with shared moorings". *Ocean Engineering,* ***171***, pp. 172–180.

[7] Faltinsen, O., 1993. *Sea loads on ships and offshore structures*, Vol. 1. Cambridge university press.

[8] Irvine, H., 1992. *Cable Structures*. Dover Publications.

[9] DNV GL, 2019. Sesam user manual, wave analysis by diffraction and morison theory. Høvik, Norway.

[10] SINTEF Ocean, 2019. SIMO 4.16.0 User Guide. Trondheim, Norway.

[11] SINTEF Ocean, 2019. RIFLEX 4.16.0 User Guide. Trondheim, Norway.

[12] Jonkman, J., Butterfield, S., Musial, W., and Scott, G., 2009. Definition of a 5-MW reference wind turbine for offshore system development. Tech. Rep. NREL/TP-500-38060, National Renewable Energy Lab.(NREL), Golden, CO (United States).

[13] Jonkman, J., 2010. Definition of the Floating System for Phase IV of OC3. Tech. Rep. NREL/TP-500-47535, National Renewable Energy Lab.(NREL), Golden, CO (United States).

[14] DNV GL, 2015. Offshore standard DNVGL-OS-E301, Position mooring. Høvik, Norway.

[15] DNV GL, 2015. Offshore standard DNVGL-OS-E302, Offshore mooring chain. Høvik, Norway.

[16] DNV GL, 2015. Offshore standard DNVGL-OS-E304, Offshore mooring steel wire ropes. Høvik, Norway.